J. Am. Soc. Mass Spectrom. (2019)
DOI: 10.1007/s13361-019-02237-z

FOCUS: HONORING HELMUT SCHWARZ'S ELECTION TO THE NATIONAL ACADEMY OF SCIENCES: RESEARCH ARTICLE

On the Competition Between Electron Autodetachment and Dissociation of Molecular Anions

Gerd Marowsky,[1] Jürgen Troe,[1,2,3] Albert A. Viggiano[4]

[1]Laser-Laboratorium Göttingen, Hans-Adolf-Krebs-Weg 1, 37077, Göttingen, Germany
[2]Institut für Physikalische Chemie, Universität Göttingen, Tammannstrasse 6, 37077, Göttingen, Germany
[3]Max-Planck-Institut für Biophysikalische Chemie, Am Fassberg 11, 37077, Göttingen, Germany
[4]Air Force Research Laboratory, Space Vehicles Directorate, 3550 Aberdeen Avenue SE, Bldg 570, Kirtland Air Force Base, Albuquerque, NM 87117-5-776, USA

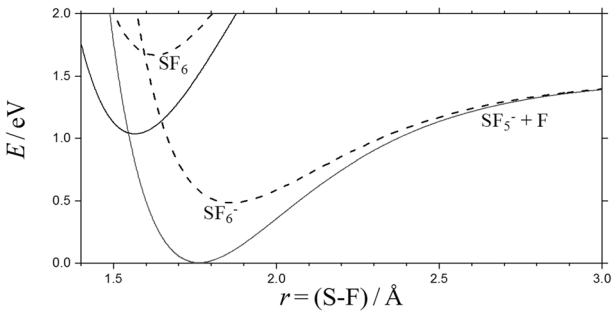

Abstract. We treat the competition between autodetachment of electrons and unimolecular dissociation of excited molecular anions as a rigid-/loose-activated complex multichannel reaction system. To start, the temperature and pressure dependences under thermal excitation conditions are represented in terms of falloff curves of separated single-channel processes within the framework of unimolecular reaction kinetics. Channel couplings, caused by collisional energy transfer and "rotational channel switching" due to angular momentum effects, are introduced afterward. The importance of angular momentum considerations is stressed in addition to the usual energy treatment. Non-thermal excitation conditions, such as typical for chemical activation and complex-forming bimolecular reactions, are considered as well. The dynamics of excited SF_6^- anions serves as the principal example. Other anions such as CF_3^- and $POCl_3^-$ are also discussed.

Keywords: Electron autodetachment, Anion dissociation, Rotational channel switching

Received: 20 February 2019/Revised: 2 April 2019/Accepted: 22 April 2019

Introduction

Vibrationally excited molecular anions may undergo a variety of processes such as dissociation to anionic and neutral fragments, autodetachment of electrons, radiative stabilization, and collisional deactivation (or activation). The competition between these channels is governed by the energy E and the rotational state of the anion (the latter symbolically characterized by an angular momentum quantum number J). While the influence of the energy is always taken into account, angular momentum effects are often neglected. As the overall reaction represents a multichannel system, channel coupling effects also have to be accounted for. The present article intends to illustrate the competition between the various channels using thermally excited SF_6^- anions as the main example. Other anions are considered as well. Finally, non-thermal excitation conditions are discussed with respect to angular momentum effects.

At sufficiently high energies, vibrationally excited anions SF_6^{-*} may react by

$$SF_6^{-*} \rightarrow SF_5^- + F \quad (1)$$

$$SF_6^{-*} \rightarrow SF_6 + e^- \quad (2)$$

$$SF_6^{-*} \rightarrow SF_6^- + h\nu \quad (3)$$

Correspondence to: Jürgen Troe; *e-mail:* shoff@gwdg.de

Published online: 28 May 2019

$$SF_6^{-*} + M \rightarrow SF_6^- + M \quad (4)$$

$$SF_6^- + M \rightarrow SF_6^{-*} + M \quad (5)$$

At even higher energies, the additional dissociation

$$SF_6^{-*} \rightarrow SF_5 + F^- \quad (6)$$

may be included. Reaction (1) corresponds to a simple bond fission with a loose activated complex (AC) which is located at the centrifugal maximum of an ion-induced dipole potential (plus some valence contributions, see, e.g., [1, 2]). In contrast to Reaction (1), Reaction (2) effectively involves a rigid AC, located at the crossing of the SF_5^--F and SF_5-F potential curves [3–6]. Figure 1 illustrates this crossing for the non-rotating and rotating SF_6^-/SF_6 system in comparison to the potential of the dissociating anion SF_6^-. The crossing in the SF_6^-- system probably involves a small energy barrier, but even without that barrier, the crossing occurs at a more compact nuclear configuration of SF_6^- than that relevant for Reaction (1). Considering the nuclear motion only, the system then is of rigid-AC/loose-AC character (one has to note, however, that nuclear and electronic motions in this description are separated which is an essential element of the "kinetic modeling approach" as justified later on).

One of the consequences of the rigid-AC/loose-AC character is markedly different J dependences of the channel threshold energies $E_{0,i}$ (the subscript $i = 1$ corresponds to the dissociation channel (1) while $i = 2$ corresponds to the detachment channel (2)). This may even lead to "rotational channel switching" [8, 9] of channels (1) and (2). While $E_{0,1}(J = 0)$ is larger than $E_{0,2}(J = 0)$, at some value of J (denoted by J_{sw}), the ordering of the $E_{0,i}$ may change from $E_{0,1}(J) > E_{0,2}(J)$ for $J < J_{sw}$ to $E_{0,1}(J) < E_{0,2}(J)$ for $J > J_{sw}$. As this is also of relevance for non-thermal conditions, this effect will be further explored below.

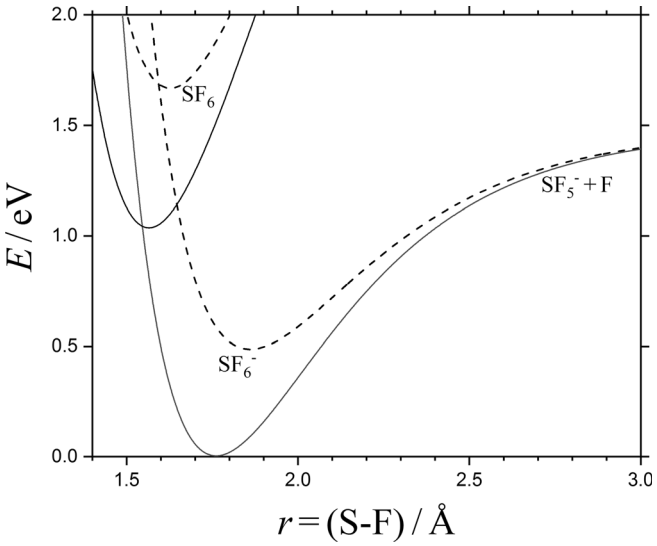

Figure 1. Potential curves for $SF_6 \rightarrow SF_5 + F$ and $SF_6^- \rightarrow SF_5^- + F$ at $J = 0$ (full lines) and $J = 250$ (dashed lines) (Morse potentials with exponentially damped centrifugal energies and data from [4, 7], leading to $E_{0,1}(J = 0) \approx 1.44$ eV and $E_{0,1}(J = 250) \approx 0.90$ eV for dissociation of SF_6^-, and $E_{0,2}(J = 0) \approx E_{0,2}(J = 250) \approx 1.03$ eV for electron detachment from SF_6^-)

The branching fraction of the reaction

$$R(SF_5^-) = [SF_5^-]/([SF_5^-] + [SF_6^-]) \quad (7)$$

may be derived from a master equation simulation of the multilevel system symbolized by Reactions (1)–(6). This simulation leads to "falloff curves" (i.e., dependences of the rate constants at fixed temperature T on the bath gas concentration [M]) of both the overall thermal dissociation rate constants k_{dis} (defined by the rate law $d[SF_5^-]/dt = k_{dis}[SF_6^-]$) and the overall detachment rate constants k_{det} (defined by the rate law $d[e^-]/dt = k_{det}[SF_6^-]$). First, these falloff curves may be calculated for "separated channels" (e.g., with the channels (1), (4), and (5) for k_{dis} and with the channels (2), (4), and (5) for k_{det}). Afterward, proper modeling requires channel coupling effects to be taken into account [10]. It is emphasized that the SF_6^--system is not unique in this regard; other anion fragmentation processes will behave in an analogous way.

Falloff Curves for Separated Electron Detachment and Dissociation Processes of SF_6^-

Falloff curves for non-dissociative electron attachment to SF_6 (in the presence and absence of radiative stabilization (3)) have been elaborated within the "kinetic modeling approach" of [11]. The rate coefficients k_{at} were determined for equal electron and bath gas temperatures T between 200 and 1400 K and for bath gas concentration $[N_2]$ between 10^{10} and 10^{20} cm^{-3}. Like other falloff curves, these can be represented in the form [12]

$$k/k_\infty = [x/(1 + x)]\ F(x) \quad (8)$$

with rate coefficients k, limiting high-pressure rate coefficients k_∞, limiting low-pressure rate coefficients k_0 (being proportional to $[N_2]$ and of the same dimension as k_∞), $x = k_0/k_\infty$, and "broadening factors" $F(x)$ approximated by

$$\log F(x) \approx \{\log F_{cent}\} / \left\{1 + [(\log x)/N]^2\right\} \quad (9)$$

where $F_{cent} = F(x = 1)$ and $N = 0.75–1.27 \log F_{cent}$ (where log = ^{10}log). Taking advantage of the modeling of $k_{at,0}$, $k_{at,\infty}$, and $F_{at,cent}$ for electron attachment of [11] and inserting these values for k_0, k_∞, and F_{cent} into Eq. (8), k_{at} is obtained. It then can be converted into thermal rate coefficients for detachment k_{det}, employing the corresponding equilibrium constant

$$K_{\mathrm{det}} = k_{\mathrm{det}}/k_{\mathrm{at}} = ([e^-][\mathrm{SF_6}]/[\mathrm{SF_6}^-])_{\mathrm{eq}} \quad (10)$$

The following parameters were calculated for the falloff curves of k_{at} (without radiative stabilization (3)): $k_{\mathrm{at},0} \approx [\mathrm{N_2}]\ 2.5 \times 10^{-18}\ \exp(-T/80\ \mathrm{K})\ [1 + 3.5 \times 10^{-22}\ (T/\mathrm{K})^7]\ \mathrm{cm^6\ s^{-1}}$, $k_{\mathrm{at},\infty} \approx 2.2 \times 10^{-7}\ (T/500\ \mathrm{K})^{-0.35}\ \mathrm{cm^3\ s^{-1}}$, and $F_{\mathrm{at,cent}} \approx \exp(-T/520\ \mathrm{K})$ [11, 13].

Since the publication of [11, 13], the electron affinity EA of SF_6 has been disputed [4, 7, 14–17]. As K_{det} and k_{det} both include a factor $\exp(-\mathrm{EA}/k_{\mathrm{B}}T)$, the value of EA is of primary importance for these two quantities. In addition to EA, also the vibrational partition function Q_{vib} (SF_6^-) had to be modified [7], because marked anharmonicities of the vibrations of SF_6^- were discovered in [4]. These refinements influence not only K_{det}, k_{det}, and k_{at} but also the falloff curves for dissociating SF_6^-. This is illustrated in the following.

Falloff curves for k_{dis}, i.e., for the dissociation of SF_6^- to $SF_5^- + F$, are also represented in the form of Eq. (8). In this case, it appears appropriate to start with the limiting high-pressure rate coefficients $k_{\mathrm{rec},\infty} \approx 2.15 \times 10^{-10}\ \mathrm{cm^3\ s^{-1}}$ for combination of an ion with a neutral species in a charge-induced dipole potential (see [13]; $k_{\mathrm{rec},\infty}$ here is assumed to be independent of the temperature). With the corresponding equilibrium constant,

$$K_{\mathrm{dis}} \approx k_{\mathrm{dis}}/k_{\mathrm{rec}} = ([\mathrm{SF_5}^-][\mathrm{F}]/[\mathrm{SF_6}^-])_{\mathrm{eq}} \quad (11)$$

this leads to $k_{\mathrm{dis},\infty}$. On the other hand, the limiting low-pressure rate coefficient $k_{\mathrm{dis},0}$ can directly be calculated from the unimolecular rate theory as elaborated in [12]. Analogous to K_{det} and k_{det}, both K_{dis} and k_{dis} include a factor $\exp[-\mathrm{EA}/k_{\mathrm{B}}T]$. In addition, however, they include the factor $\exp[-\Delta E_0/k_{\mathrm{B}}T]$ where ΔE_0 corresponds to the energy difference between $SF_6 + e^-$ and $SF_5^- + F$ at 0 K (being 0.41 eV [7]). Furthermore, K_{dis} and k_{dis} include the strongly anharmonic vibrational partition function $Q_{\mathrm{vib}}(SF_6^-)$. Analogous to the dispute about the EA of SF_6, the energy difference ΔE_0 has multiple values in the literature (see, e.g., [3, 7, 13, 14, 18–23]). (The dissociation channel (6) of SF_6^-*requires higher energies than SF_5^- formation [22] and, therefore, is not further considered here.) In view of the difficulties with EA, ΔE_0, and Q_{vib} (SF_6^-), it appears important to analyze to what extent the modeled rate constants become independent of these difficulties, because some of the uncertainties compensate each other.

The largest uncertainties encountered in the modeling of $k_{\mathrm{dis},0}$ can be estimated within the formulation of the unimolecular rate theory described in [12]. $k_{\mathrm{dis},0}$ contains a factor $\rho_{\mathrm{vib,h}}\ (\mathrm{EA} + \Delta E_0)\ F_{\mathrm{anh}}/Q_{\mathrm{vib}}$ for SF_6^-, where $\rho_{\mathrm{vib,h}}\ (\mathrm{EA} + \Delta E_0)$ denotes the harmonic vibrational density of states and F_{anh} is an anharmonicity factor. The anharmonicity contributions in Q_{vib} and the factor F_{anh} in part compensate each other. However, the anharmonicity in Q_{vib} has been essential in the third-law evaluation by [7] of the experimental ratio $k_{det}/k_{at} = K_{\mathrm{det}}$, leading to the electron affinity EA = 1.03(± 0.05) eV. It should be mentioned that this value was supported by the most detailed quantum chemical calculations of [15]. In the modeling of $k_{\mathrm{dis},0}$, besides $\mathrm{EA} + \Delta E_0$ and the ratio $\rho_{\mathrm{vib,h}}\ (\mathrm{EA} + \Delta E_0)\ F_{\mathrm{anh}}/Q_{\mathrm{vib}}$, the average energy $\langle \Delta E_{\mathrm{coll}} \rangle$ transferred per collision between SF_6^-* and M remains an uncertain parameter. Keeping in mind these uncertainties and leaving a fine-tuning of $k_{\mathrm{dis},0}$ to the comparison with the experiments, we model $k_{\mathrm{dis},0}$ with the harmonic frequencies of SF_6^- from [24] (such as given in [13]), EA = 1.03 eV from [7], a total collisional energy transfer frequency approximated by the Langevin collision frequency $Z = 6.37 \times 10^{-10}\ \mathrm{cm^3\ s^{-1}}$ (for collisions between SF_6^{-*} and N_2 [14]) and $\langle \Delta E_{\mathrm{coll}} \rangle / \mathrm{hc} \approx -200\ \mathrm{cm^{-1}}$ [25, 26]. This leads to

$$k_{\mathrm{dis},0} \approx [\mathrm{N_2}]\ 4.3 \times 10^{-3} (T/650\ \mathrm{K})^{-11.6} \exp\left[-(\mathrm{EA} + \Delta E_0)/k_{\mathrm{B}}T\right]\ \mathrm{cm^3 s^{-1}} \quad (12)$$

While $k_{\mathrm{dis},0}\ (T)$ relies on modeling, $k_{\mathrm{det},0}$ directly follows from the experimental $k_{\mathrm{at},0}$ [7] and the revised K_{det} from [7], one obtains

$$k_{\mathrm{det},0} \approx [\mathrm{N_2}]\ 3.4 \times 10^{-5} (T/650\ \mathrm{K})^{-8.9} \exp\left[-\mathrm{EA}/k_{\mathrm{B}}T\right]\ \mathrm{cm^3 s^{-1}} \quad (13)$$

Around 650 K, where measurements of the branching fraction $R(SF_5^-)$ are available [13, 14, 27, 28], obviously $k_{\mathrm{det},0}$ is much larger than $k_{\mathrm{dis},0}$, i.e., $k_{\mathrm{det},0} > k_{\mathrm{dis},0}$. This is in contrast to $k_{\mathrm{dis},\infty}$ and $k_{\mathrm{det},\infty}$ where the former is given by

$$k_{\mathrm{dis},\infty} \approx 1.5 \times 10^{15} (T/650\ \mathrm{K})^{-1} \exp\left[-(\mathrm{EA} + \Delta E_0)/k_{\mathrm{B}}T\right]\ \mathrm{s^{-1}} \quad (14)$$

while the latter amounts to

$$k_{\mathrm{det},\infty} \approx 1.1 \times 10^{10} (T/650\ \mathrm{K})^{-1.4} \exp\left[-\mathrm{EA}/k_{\mathrm{B}}T\right]\ \mathrm{s^{-1}} \quad (15)$$

such that $k_{\mathrm{dis},\infty} > k_{\mathrm{det},\infty}$. The comparison of the pre-exponential factors of Eqs. (14) and (15) classifies detachment as an effectively rigid-AC process and supports the view of the "kinetic modeling approach" given in the "Introduction." On the other hand, dissociation is clearly a loose-AC bond fission reaction. The observation of $k_{\mathrm{dis},0} < k_{\mathrm{det},0}$ and $k_{\mathrm{dis},\infty} > k_{\mathrm{det},\infty}$ (near 650 K) indicates that there must be a crossing of the two falloff curves at some $[N_2]$ (denoted by $[N_2]_x$ or by the corresponding bath gas pressure p_x). In order to locate p_x, we also need F_{cent} which, for simplicity, we use in the form $F_{\mathrm{dis,cent}} \approx F_{\mathrm{at,cent}}$ as calculated in [11]. Figure 2 illustrates pairs of falloff curves for 600, 650, and 700 K. The curves cross near $[N_2]_x \approx 1.5 \times 10^{15}\ \mathrm{cm^{-3}}$ (corresponding to $p_x \approx 0.1$ Torr). At this pressure, dissociation is close to its low-pressure limit while detachment is closer to

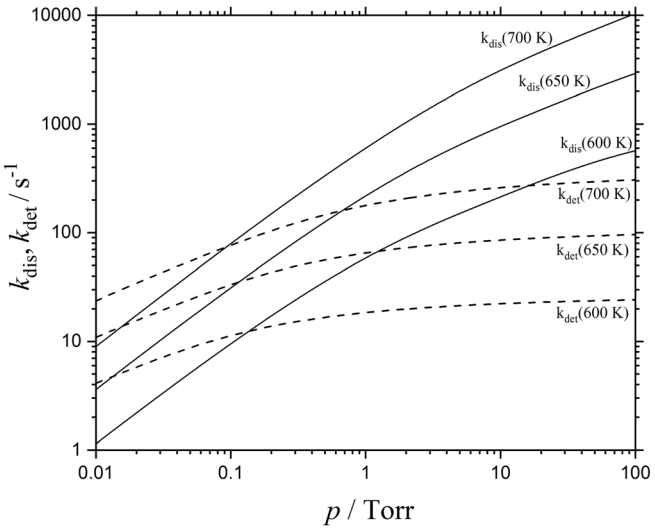

Figure 2. Falloff curves for autodetachment of electrons (dashed curves) and dissociation (full curves) of thermally excited SF_6^- anions at 600, 650, and 700 K

its high-pressure limit. Figure 3 shows the corresponding branching fraction $R(SF_5^-)$ for $T = 650$ K, being constructed with $R(SF_5^-) = k_{dis}/(k_{dis} + k_{det})$ from Figure 2 (it should be mentioned that Figure 3 is consistent with Figures 8 and 9 of [14]). As the exponential factor $\exp[-\Delta E_0/k_B T]$ dominates $R(SF_5^-)$, while other not so well-known contributions have only weaker temperature dependences, the evaluation of the temperature dependence of $R(SF_5^-)$ provides safe access to ΔE_0. This formed the basis for the fit of $\Delta E_0 \approx 0.41$ eV in [7, 29]. However, channel coupling effects were neglected so far. Therefore, one has to make sure that rotational channel switching and the related multichannel coupling effects do not matter too much. In the following section, we explore to what extent the rigid-AC/loose-AC multichannel character of the system requires multichannel coupling corrections.

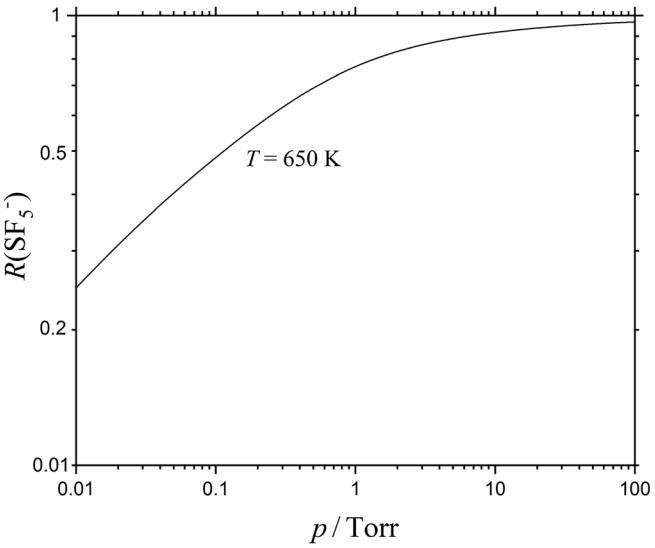

Figure 3. Branching fractions $R(SF_5^-) = [SF_5^-]/([SF_5^-] + [SF_6^-]) = k_{dis}/(k_{dis} + k_{det})$ for reaction of thermally excited SF_6^- anions at 650 K (with k_{dis} and k_{det} from Figure 2)

Rotational Channel Switching and Multichannel Coupling Effects in SF_6^-

The foregoing section provided falloff curves for separated electron detachment and dissociation of thermally excited SF_6^-. It illustrated that electron detachment in the language of "kinetic modeling" effectively proceeds as a rigid-AC process whereas dissociation is a loose-AC process. In this situation, rotational channel switching, such as described in the "Introduction," modifies the branching fractions which—so far—were calculated assuming separated, single-channel, falloff curves.

The rigid AC of the electron detachment process is located at the nuclear configuration where the potential curves of SF_5-F and $(SF_5\text{-}F)^-$ cross (see Figure 1). This crossing happens at an S-F distance $r_x \approx 1.58$ Å which corresponds to a structure with an effective rotational constant $B_e\,(r_e/r_x)^2 \approx B_e$ (B_e is the rotational constant, being 0.0907 cm^{-1} for SF_6 and 0.0750 cm^{-1} for SF_6^-, while $r_e \approx 1.56$ Å for SF_6 and 1.76 Å for SF_6^-). The threshold energy $E_{det,0}$ (J) for rotating SF_6^- then roughly increases as

$$E_{0,det}(J) \approx E_{0,det}(J = 0) + B_e h\, c\, J\,(J + 1) \tag{16}$$

where

$$E_{0,det}(J = 0) \approx EA + 5.2\ \text{meV} \tag{17}$$

(a barrier of about 5.2 meV in [5] was fitted with the help of the low-temperature experiments of [6]; however, this value is only of little relevance for the estimate of J_{sw}). The threshold energies $E_{0,dis}$ (J) correspond to the centrifugal barriers in the $(SF_5^-\text{-}F)$ potential and can be estimated for an ion-induced dipole potential as shown in [1]. As the second term of Eq. (17) and the extra energy due to the centrifugal maxima in the dissociation process in excess of the energy $EA + \Delta E_0$ are both small compared to ΔE_0, they are neglected here. The switching value J_{sw} then follows from the relationship

$$B_e h\, c J_{sw}(J_{sw} + 1) \approx \Delta E_0 \tag{18}$$

With $\Delta E_0 \approx 0.41$ eV, this leads to

$$J_{sw} \approx 191 \tag{19}$$

For $J > J_{sw}$, $E_{0,det}$ (J) becomes larger than $E_{0,dis}$ (J), i.e., rotational channel switching occurs and rotationally hot SF_6^- has a smaller threshold energy for dissociation than for electron detachment.

Rotational channel switching is the dominant cause for channel coupling in rigid-AC/loose-AC, two-channel, reaction systems [10]. Branching fractions R_1 for the energetically less

favorable channel (at $J = 0$; R_1 corresponds to the energetically less favorable channel) are defined by $R_1 = k_1/(k_1 + k_2)$. At a given temperature, R_1 varies with the bath gas concentration [M]. It increases from a limiting low-pressure value of $R_{1,0}$ to a limiting high-pressure value of $R_{1,\infty}$. This increase can be represented in approximate form by

$$R_1 \approx R_{1,0} + \left(R_{1,\infty} - R_{1,0}\right) x/(x+1) \tag{20}$$

where $x = [\mathrm{M}]/[\mathrm{M}]_{\mathrm{cent}}$ ($[\mathrm{M}]_{\mathrm{cent}}$ denotes that [M] for which $x = 1$ in Eq. (8)). The limiting low-pressure value $R_{1,0}$ is related to J_{sw} by

$$R_{1,0} \approx \exp\left[-\mathrm{B_e hc}\, J_{\mathrm{sw}}(J_{\mathrm{sw}}+1)/\mathrm{k_B}T\right] \tag{21}$$

For SF_6^-, this leads to $R_{1,0} \approx \exp(-4760\ \mathrm{K}/T)$. Channel coupling effects, therefore, only become important at very high temperatures for the present case. Branching fractions $R(SF_5^-)$, corresponding to R_1, at lower temperatures, thus can be calculated with the separated channel rate constants $k_{\mathrm{det}}([\mathrm{M}])$ and $k_{\mathrm{dis}}([\mathrm{M}])$ (and $[\mathrm{M}]_{\mathrm{cent}} \approx [\mathrm{N_2}]_x$ as shown in Figure 3) while channel coupling effects remain negligible. The results of the previous section (as illustrated by Figure 3), therefore, were not "contaminated" by rotational channel switching and channel coupling effects.

Non-thermal Activation Conditions

It has to be emphasized that the described analysis of channel coupling effects in terms of Eq. (20) applies to thermal energy and angular momentum distributions only. In many experiments, however, the anions are produced with non-thermal distributions. For example, dissociative electron attachment (DEA) experiments start with non-thermal distributions of the states of the anions. These relax toward thermal distributions only in the presence of collisions. DEA then behaves as a "chemical activation system." The corresponding relaxation of the branching fractions $R(SF_5^-)$ toward their equilibrium values has been followed experimentally in [14]. For the time during the relaxation, master equation simulations have to describe the competition between the reaction steps (1)–(3) and the collision processes (4) and (5). The yields of the corresponding chemical or photochemical activation systems as a function of the primary excitation energy and the bath gas pressure have been modeled in [27]. The results can directly be applied to DEA. Meanwhile, the uncertainty in the value of $\langle \Delta E_{\mathrm{coll}} \rangle$ for collisional energy transfer and, in particular, of the change of the angular momentum distribution during the collisional relaxation limits the accuracy of the simulation. Further work is required to analyze the consequences of rotational channel switching under non-thermal activation conditions which are certainly different from those of the thermal excitation analyzed here. Finally, the analogy of the chemical activation situation to the pressure and temperature dependence of complex-forming bimolecular reactions should be stressed, such that the approximate expressions for yields from the corresponding treatment may become helpful [28].

Apart from rotational channel switching in rigid-AC/loose-AC multichannel systems, also "vibrational channel switching," particularly under non-thermal excitation conditions, is of importance [9]. The specific rate constants $k_{\mathrm{dis}}(E,J)$ for fixed J at some energy E_{sw} then cross the corresponding $k_{\mathrm{det}}(E,J)$. This was illustrated, e.g., for DEA of SF_6^- at $J = 0$ in Figure 5 of [13]. Under thermal excitation conditions, this effect is responsible for the markedly different preexponential factors of $k_{\mathrm{dis},\infty}(T)$ and $k_{\mathrm{det},\infty}(T)$ in Eqs. (14) and (15). Under non-thermal excitation conditions and in the absence of collisions, the differences of the $k(E,J)$ will cause quite different time dependences of the decaying anions. Energy and angular momentum as well as channel switching effects then will all have to be taken into account. Oversimplification of the multichannel character of the process and its energy and angular momentum dependence may have been the reason for different interpretations of experiments (possibly also for the different values derived for EA of SF_6 in [4, 7, 14–17]).

Systems with Loose-AC/Rigid-AC and Rigid-AC/Rigid-AC Channels

Analogous to the SF_6^- example, one should inspect rotational channel switching effects in other DEA systems. First, we consider the CF_3^- example where

$$CF_3^- * \rightarrow CF_3 + e^- \tag{22}$$

$$CF_3^- * \rightarrow F^- + CF_2 \tag{23}$$

compete. With an electron affinity of EA = 1.82 (± 0.05) eV for CF_3 [30] and an energy difference $\Delta E_0 = 0.22$ (± 0.02) eV [31], this system according to Eq. (18) has a smaller J_{sw} than SF_6^-. The crossing between the $(CF_2\text{-}F)$ and $(CF_2\text{-}F)^-$ potential curves here takes place at $r_x \approx r_e$ [32], such that $J_{\mathrm{sw}} \approx 70$ (with $B_e \approx 0.360\ \mathrm{cm}^1$). This confirms again a loose-AC/rigid-AC character of the system. Experimental studies of the DEA to CF_3 [32, 33] so far have only been concerned with the chemical activation regime of the process, and rotational channel switching effects were not yet considered. If the process would have been followed over the relaxation period from chemical activation to thermal distributions, the branching fraction would have been characterized by Eq. (20) with $R_{1,0} \approx \exp(-2570\ \mathrm{K}/T)$. Obviously, this would have been relevant for temperatures which were beyond those considered so far. However, as emphasized above, channel switching effects are important as well during the relaxation stage typically achieved in DEA experiments.

Multichannel coupling effects caused by rotational channel switching are ubiquitous, e.g., in DEA to other fluorocarbon radicals [34], in DEA to CF_3Br [33], or in DEA to $POCl_3$ [35–37]. The latter system could be affected by rotational channel switching in particular, as small values of ΔE_0 are observed ($\Delta E_0 \approx 0$ for the production of $POCl_2^- + Cl$ and $\Delta E_0 = 0.11$ eV for the production of $POCl_2 + Cl^-$). The preliminary modeling with a chemical activation scheme here was successful under the assumption of a loose AC for the $POCl_2 + Cl^-$ channel while a more rigid AC was found for the $POCl_2^- + Cl$ channel. The presence of several competing channels with different individual J_{sw} further complicates the analysis. In this case, branching fractions under thermal and non-thermal conditions may take advantage of the multichannel codes elaborated in [10].

One observation from the analysis of the experiments on the $POCl_3$ system in [37] deserves further attention. Assuming a loose-AC character for all dissociation channels, "rigidity factors" f_{rigid} in that analysis were fitted. These factors account for an anisotropy of the potential beyond the isotropy of the dominant ion-induced dipole potential between the dissociation fragments. This fitting in [37] led to markedly smaller values of f_{rigid} for the nearly thermoneutral $POCl_2^- + Cl$ channel than for the endothermic $POCl_2 + Cl^-$ channel. This observation may suggest that the former channel involves some intermediate energy barrier. This might signal rigid-AC channel behavior of this dissociation channel. Multichannel coupling effects under thermal conditions for rigid-AC/rigid-AC then would be characterized by Eq. (20) with

$$R_{1,0} \approx \exp\left(-\Delta E_0/\gamma\right) \tag{24}$$

where γ denotes the average energy transferred per up collision (related to the total $<\Delta E_{coll}>$ by $<\Delta E_{coll}>/hc = \gamma - \alpha$ where $\gamma \approx \alpha k_B T/(\alpha + k_B T$; α and γ traditionally are given in cm^{-1}) and α is the average energy transferred per down collision). In this case, instead of rotational channel switching, collisional processes would be responsible for multichannel coupling effects.

Conclusions

The present article characterizes the competition between electron autodetachment and fragmentation of vibrationally excited molecular anions in the language of chemical kinetics. The main conclusion consists in the statement that autodetachment of electrons effectively corresponds to a rigid-activated complex process, while fragmentations mostly have loose activated complexes (although sometimes the latter also may be governed by rigid-activated complexes). A rigid-AC/loose-AC character of the reaction gives rise to rotational channel switching where energetically less favorable reaction channels dominate over energetically more favorable channels when the ion rotates rapidly. In the presence of collisions, also multichannel coupling effects have to be taken into account. The branching fractions under thermal excitation conditions can be represented approximately by Eqs. (18), (20), and (21). The importance of energy and angular momentum effects under non-thermal, chemical-activation type, excitation conditions is stressed as well.

Acknowledgements

Open access funding provided by Max Planck Society. The authors have been inspired by the seminal work of Professor Helmut Schwarz and are grateful for numerous interactions over many years. J.T. acknowledges support by EOARD Grant Award No FA9550-17-1-0181 and A.A.V. by the Air Force Office of Scientific Research (AFOSR-19RVCOR042). We are grateful for technical help by A. Maergoiz.

Open Access

References

1. Troe, J.: Statistical adiabatic channel model of ion-neutral dipole capture rate constants. Chem. Phys. Lett. **122**, 425–430 (1985)
2. Troe, J., Ushakov, V.G., Viggiano, A.A.: SACM/CT study of product energy distributions in the dissociation of *n*-propylbenzene cations. Z. Phys. Chem. **219**, 699–714 (2005)
3. Gerchikov, L.G., Gribakin, G.F.: Electron attachment to SF_6 and lifetimes of SF_6^- negative ions. Phys. Res. A. **77**, 042724 (2008)
4. Eisfeld, W.: Highly accurate determination of the electron affinity of SF_6 and analysis of structure and photodetachment spectrum of SF_6^-. J. Chem. Phys. **134**, 054303 (2011)
5. Troe, J., Marowsky, G., Shuman, N.S., Miller, T.M., Viggiano, A.A.: On the temperature dependence of the thermal electron attachment to SF_6, SF_5Cl, and $POCl_3$. Z. Phys. Chem. **225**, 1405–1416 (2011)
6. Le Garrec, J.L., Sidko, O., Queffelec, J.L., Hamon, S., Mitchel, J.B.A., Rowe, B.R.: Experimental studies of cold electron attachment to SF_6, CF_3Br, and CCl_2F_2. J. Chem. Phys. **107**, 54–63 (1997)
7. Troe, J., Miller, T.M., Viggiano, A.A.: Revised electron affinity of SF_6 from kinetic data. J. Chem. Phys. **136**, 121102 (2012)
8. Troe, J.: Rotational effects in complex-forming bimolecular reactions: application to the reaction $CH_4 + O_2^{+*}$. Int. J. Mass Spectrom. **80**, 17–30 (1987)
9. Troe, J.: The colourful world of complex-forming bimolecular reactions. J. Chem. Soc. Faraday Trans. **90**, 2303–2317 (1994)
10. Troe, J.: Simplified analysis and representation of multichannel thermal unimolecular reactions. J. Phys. Chem. A. **123**, 1007–1014 (2019)
11. Troe, J., Miller, T.M., Viggiano, A.A.: Low-energy electron attachment to SF_6. I. Kinetic modeling of nondissociative attachment. J. Chem. Phys. **127**, 244303 (2007)
12. Troe, J.: Predictive possibilities of unimolecular rate theory. J. Phys. Chem. **83**, 114–126 (1979)
13. Viggiano, A.A., Miller, T.M., Friedman, J.F., Troe, J.: Low-energy electron attachment to SF_6 III. From thermal detachment to the electron affinity of SF_6. J. Chem. Phys. **127**, 244305 (2007)
14. Troe, J., Miller, T.M., Viggiano, A.A.: Low-energy electron attachment to SF_6. II. Temperature and pressure dependences of dissociative attachment. J. Chem. Phys. **127**, 244304 (2007)

15. Karton, A., Martin, J.M.L.: Comment on "Revised electron affinity of SF_6 from kinetic data" [J. Chem. Phys. 136, 121102 (20112)]. J. Chem. Phys. **136**, 197101 (2012)
16. Menk, S., Das, S., Blaum, K., Froese, M.W., Lange, M., Mukherjee, M., Repnow, R., Schwalm, D., von Hahn, R., Wolf, A.: Vibrational autodetachment of sulfur hexafluoride anions at its long-lifetime limit. Phys. Rev. A. **89**, 022502 (2014)
17. Luzon, I., Nagler, M., Heber, O., Strasser, D.: SF_6^- photodetachment near the adiabatic limit. Phys. Chem. Chem. Phys. **17**, 7670 (2015)
18. Miller, T.M., Arnold, S.T., Viggiano, A.A.: G3 and G2 thermochemistry of sulfur fluoride neutrals and anions. Int. J. Mass Spectrom. **227**, 413–420 (2003)
19. Lobring, K.C., Check, C.E., Gilbert, T.M., Sunderlin, L.S.: New measurements of thermochemistry of SF_5^- and SF_6^-. Int. J. Mass Spectrom. **227**, 361–372 (2003)
20. Graupner, K., Field, T.A., Mauracher, A., Scheier, P., Bacher, A., Denifl, S., Zappa, F., Märk, T.D.: Fragmentation of metastable SF_6^{-*} ions with microsecond lifetimes in competition with autodetachment. J. Chem. Phys. **128**, 104304 (2008)
21. Steill, J.D., Oomens, J., Eyler, J.R., Compton, R.N.: Gas-phase infrared multiple photon dissociation spectroscopy of isolated SF_6^- and SF_5^- anions. J. Chem. Phys. **129**, 244302 (2008)
22. Braun, M., Marienfeld, S., Ruf, M.-W., Hotop, H.: High-resolution electron attachment to the molecules CCl_4 and SF_6 over extended energy ranges with the (EX)LPA method. J. Phys. B Atomic Mol. Phys. **42**, 125202 (2009)
23. Akhgarnusch, A., Höckendorf, R.F., Beyer, M.K.: Thermochemistry of the reaction of SF_6 with gas-phase hydrated electrons: a benchmark for nanocalorimetry. J. Phys. Chem. A. **119**, 9978–9985 (2015)
24. Morokuma, K.: as cited in [14]
25. Fernandez, A.I., Viggiano, A.A., Miller, T.M., Williams, S., Dotan, I., Seeley, J.V., Troe, J.: Collisional stabilization and thermal dissociation of highly vibrationally excited $C_9H_{12}^+$ ions from the reaction $O_2^+ + C_9H_{12}$. J. Phys. Chem. A. **108**, 9652–9659 (2004)
26. Kim, H., Bhandari, H.N., Pratikar, S., Hase, W.L.: Chemical dynamics simulation of energy transfer: Propylbenzene cation and N_2 collisions. J. Phys. Chem. A. **123**, 2301–2309 (2019)
27. Troe, J.: Approximate expressions for the yields of unimolecular reactions with chemical and photochemical activation. J. Phys. Chem. **87**, 1800–1804 (1983)
28. Troe, J.: Simplified representation of partial and total rate constants of complex-forming bimolecular reactions. J. Phys. Chem. A. **119**, 12159–12165 (2015)
29. Kerkines, I.S.K, Morokuma, K., Bobadova-Parvanova, P.: as cited in [14]
30. Deyerl, H.-J., Alconel, L.S., Continetti, R.E.: Photodetachment imaging studies of the electron affinity of CF_3. J. Phys. Chem. A. **105**, 552–557 (2001)
31. Csontos, J., Rolik, Z., Das, S., Kallay, M.: High-accuracy thermochemistry of atmospherically important fluorinated and chlorinated methane derivatives. J. Phys. Chem. A. **114**, 13093–13103 (2010)
32. Shuman, N.S., Miller, T.M., Friedman, J.F., Viggiano, A.A., Maergoiz, A.I., Troe, J.: Pressure and temperature dependence of dissociative and non-dissociative electron attachment to CF_3: experiments and kinetic modeling. J. Chem. Phys. **135**, 054306 (2011)
33. Shuman, N.S., Miller, T.M., Viggiano, A.A., Troe, J.: Electron attachment to CF_3 and CF_3Br at temperatures up to 890 K: experimental test of the kinetic modeling approach. J. Chem. Phys. **138**, 204316 (2013)
34. Shuman, N.S., Miller, T.M., Viggiano, A.A.: Electron attachment to fluorocarbon radicals. J. Chem. Phys. **137**, 214318 (2012)
35. Van Doren, J.M., Friedman, J.F., Miller, T.M., Miller, T.M., Viggiano, A.A., Denifl, S., Scheier, P., Märk, T.D., Troe, J.: Electron attachment to $POCl_3$: measurement and theoretical analysis of rate constants and branching ratios as a function of gas pressure and temperature, electron temperature, and electron energy. J. Chem. Phys. **124**, 124322 (2006)
36. Shuman, N.S., Miller, T.M., Viggiano, A.A., Troe, J.: Electron attachment to $POCl_3$. II. Dependence of the attachment rate coefficients on gas and electron temperature. Int. J. Mass Spectrom. **306**, 123–128 (2011)
37. Shuman, N.S., Miller, T.M., Viggiano, A.A., Troe, J.: Electron attachment to $POCl_3$ III. Measurement and kinetic modeling of branching fractions. J. Chem. Phys. **134**, 094310 (2011)